

AN ACCURATE METHOD FOR IMPEDANCE MEASUREMENT OF RFID TAG ANTENNA

S.-K. Kuo, S.-L. Chen, and C.-T. Lin

Steel and Aluminum Research and Development Department
China Steel Corporation
Hsiao Kang, Kaoshiung 81233, Taiwan

Abstract—This paper presents a method of antenna impedance measurement for RFID tag antenna based on a differential probe. The importance of accurate impedance measurement in optimal design of tag antenna, especially for the metal tags, is first addressed. Afterwards, an overview of the existing methods based on the single-ended probe and the balun probe is presented. The proposed method using the differential probe is explained based the well-known two port network model. Experiments for both balanced and unbalanced tag antenna measurement demonstrate the differential probe can provided better agreement with simulated results.

1. INTRODUCTION

RFID has been an emerging research issue in recent years. Many research topics have been studied in recent investigations, including reader antenna design [1], interference and collision problems [2, 3], as well as tag design. Because of the interference problem, achieving a successful application of RFID technology in metal industry relies heavily on the design of tag antenna. Many metal tags, such as patch [4–6], inverted-F [7, 8] and loop [9], were designed in the past few years. In order to have low profile, these metal tags usually have a “sandwich type” structure, in which a dielectric layer is placed between the bottom ground plane and the upper plate with an antenna pattern. Tag performance relies heavily on two factors, antenna gain and impedance matching [10]. Because of the insufficient bandwidth and low gain characteristics [11], accomplishing accurate impedance matching is therefore very critical for metal tags, which becomes the key factor in determining the performance. Therefore, the requirement of iterated dimension adjustment during the course of optimal antenna

design highlights the importance of accurate impedance measurement. This paper presents a method for accurate impedance measurement based on a differential probe. Section 2 introduces two existing methods employed for tag antenna measurement. The differential probe with its two-port network model is discussed in Section 3. Section 4 demonstrates the probe is able to deliver better accuracy than the two well-known techniques for both balanced and unbalanced type of tag antenna. Finally, conclusions are drawn in Section 5.

2. EXISTING METHODS FOR RFID ANTENNA IMPEDANCE MEASUREMENT

Impedance measurement of RFID tag antenna with desired accuracy has been a troublesome problem for years. Before the emerge of RFID, small antenna measurement is based on a $50\ \Omega$ system, which cannot be directly applied for RFID tag antenna due to the incompatible feed nature. An RFID strap shown in Fig. 1 has two identical pads which transmit energy into tag antenna. As the feed structure is symmetrical and electrically small, the virtual ground plane established is a mid-way plane. Therefore, an RFID strap is served as a balanced feed. Some researchers attempted to measure the tag antenna using different kinds of probes, which can be separated into two categories, single-ended probe and balun connected probe.

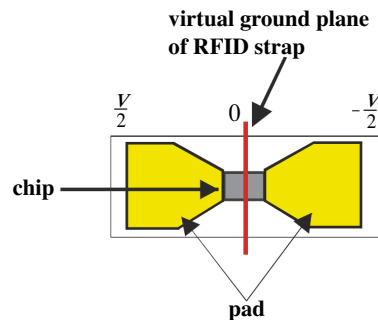


Figure 1. An RFID trap and its virtual ground surface.

2.1. Single-ended Probe

A single-ended probe is formed by connecting an extension from the coaxial cable. The extension, which can be a SMA connector [12, 13], a wafer probe [14], or other type of the structure, has two tips probing the feed of the tag antenna. Fig. 2(a) shows a commercially available probe

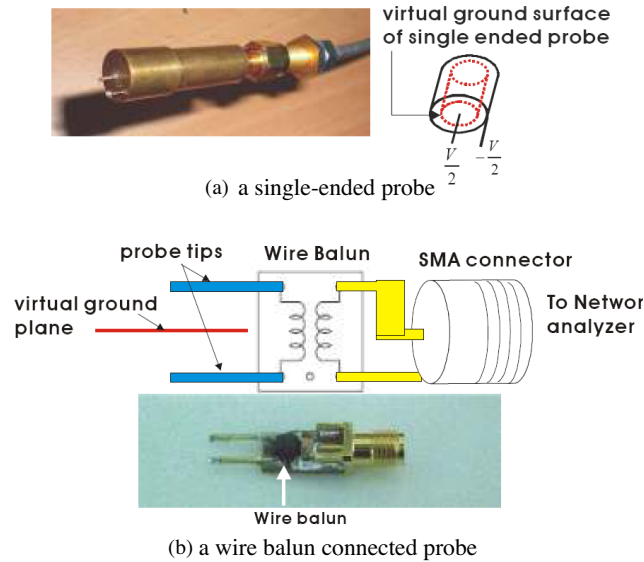


Figure 2. Existing method for RFID tag antenna measurement.

extension. Using single-ended probe for tag antenna measurement is inappropriate since the single-ended probe is an unbalanced feed. The virtual ground surface is quite close to a three dimensional cylindrical surface. When connecting a single-ended probe to a balanced tag antenna, the unbalanced nature of the probe changes the electromagnetic field distribution around the feed area. The situation might become worse when probing an unbalanced antenna. Therefore, this method cannot provide accurate measurement results.

2.2. Balun Probe

A balun is recognized as a balance-unbalance converter, which can provide differential current at its output port [15]. A wire balun has larger bandwidth than a microstrip balun, and hence has been used for tag antenna measurement [12, 16]. Fig. 2(b) shows a probe which is formed by connecting a wire balun in front of a SMA connector. Two probe tips attached to the other side of the balun are used for probing the antenna. The commercially available wire balun has a 2.5 turns coil wound around a ferrite core, offering a bandwidth around 3.3 GHz. Because the balun is inherently a transformer, it exerts equal and opposite currents at both tips. Therefore, the way it distributes the electromagnetic field is identical to an RFID strap.

3. DIFFERENTIAL PROBE AND ITS TWO-PORT NETWORK MODEL

A differential probe proposed by Palmer et al., has a symmetrical structure, and hence was employed to measure a balanced antenna [17]. It is formed by combining two ports using a fixture as shown in Fig. 3, with the metal shield of the coaxial cables connected together to be the common ground.

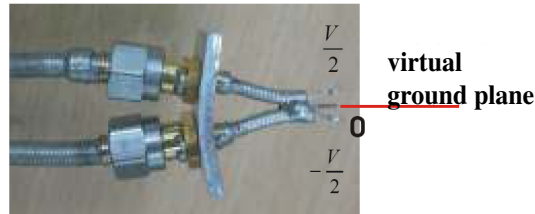


Figure 3. A differential probe and its virtual ground plane.

For the purpose of calibration, a short wire is extended from the ground as seen in Fig. 3. Performing full two-port “SOLT” (short-open-load-through) calibration establishes a calibration plane at the probe tips. Because the differential probe is basically a balanced device with its ground right in the middle of the two tips, it is appropriate for tag antenna measurement. A two-port π -network as shown in Fig. 4 is used for modeling the antenna and the probe, in which difference between Z_a and Z_b accounts for unbalance of the tag antenna.

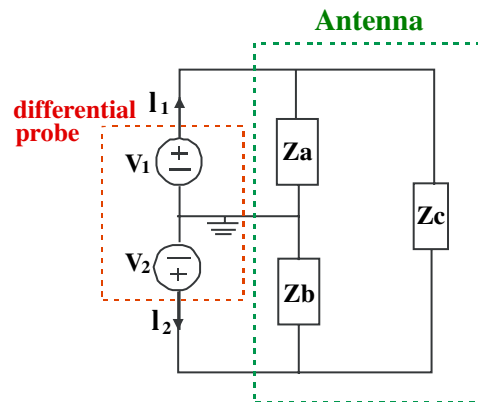


Figure 4. A two-port π -network model for the probe and antenna.

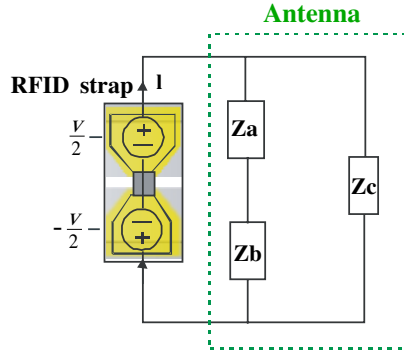


Figure 5. Network model for RFID strap and tag antenna.

Figure 5 shows when the differential probe is replaced by a RFID probe, the impedance actually “seen” by the RFID chip becomes

$$Z_{ANT} = (Z_a + Z_b) \parallel Z_c \quad (1)$$

In order to obtain Z_a , Z_b and Z_c , S -parameters S_{11} , S_{12} , S_{21} and S_{22} were obtained and then converted to Y -parameters. Afterward, Z_a , Z_b and Z_c can be calculated through following equations [17],

$$Z_a = \frac{1}{Y_{22} + Y_{21}} \quad (2a)$$

$$Z_b = \frac{1}{Y_{11} + Y_{21}} \quad (2b)$$

$$Z_c = -\frac{1}{Y_{21}} \quad (2c)$$

Measurement result obtained by the approach mentioned above is accurate, but very time consuming as it needs to download a lot of data from the network analyzer for post-processing. On the other hand, the network analyzer (HP5710B) being used is able to convert standard parameters into mixed-mode parameters in real-time. Among the mixed-mode parameters, the differential mode parameter S_{dd11} measures the return loss of the differential signal,

$$S_{dd11} = \frac{b_1 - b_2}{a_1 - a_2} \quad (3)$$

where a_1 and a_2 represents incident waves of port 1 and port 2, while b_1 and b_2 are reflected waves [18].

Converting the measured scattering parameter into impedance gives

$$Z_{dd11} = 2Z_0 \frac{1 + S_{dd11}}{1 - S_{dd11}} \quad (4)$$

where Z_0 is the characteristic impedance of the transmission cable [19].

Substitute (3) into (4) gives

$$Z_{dd11} = 2Z_0 \frac{a_1 - a_2 + b_1 - b_2}{a_1 - a_2 - b_1 + b_2} \quad (5)$$

Represent a_1 , a_2 , b_1 and b_2 by $a_i = \frac{V_i + Z_0 I_i}{\sqrt{Z_0}}$ and $b_i = \frac{V_i - Z_0 I_i}{\sqrt{Z_0}}$, for $i = 1, 2$, the impedance Z_{dd11} is expressed as

$$Z_{dd11} = 2 \frac{V_1 - V_2}{I_1 - I_2} \quad (6)$$

(6) can be regarded as differential voltage, $V_1 - V_2$, divided by the average current through the load, $\frac{I_1 - I_2}{2}$.

Since in differential mode measurement incident waves of both ports has equal amplitude and opposite phase, i.e., $a_1 + a_2 = 0$, one obtains

$$V_1 + V_2 + Z_0(I_1 + I_2) = 0 \quad (7)$$

Furthermore, the relation between voltages V_1 and V_2 , and currents I_1 and I_2 in the two port network is described by a Z -matrix,

$$\begin{aligned} V_1 &= Z_{11}I_1 + Z_{12}I_2 \\ V_2 &= Z_{21}I_1 + Z_{22}I_2 \end{aligned} \quad (8)$$

Substitute (7) and (8) into (6) yields

$$Z_{dd11} = 2 \frac{Z_0(Z_{11} - Z_{12} - Z_{21} + Z_{22}) + 2(Z_{11}Z_{22} - Z_{12}Z_{21})}{2Z_0 + Z_{11} + Z_{12} + Z_{21} + Z_{22}} \quad (9)$$

In case of a balanced antenna, in which $Z_a = Z_b$, one can derive $Z_{11} = Z_{22} = Z_a \parallel (Z_a + Z_c)$, and $Z_{12} = Z_{21} = Z_a^2 / (2Z_a + Z_c)$. Therefore, Z_{dd11} in (9) can be expressed explicitly as

$$Z_{dd11} = \frac{2Z_c Z_a}{2Z_a + Z_c} \quad (10)$$

in which $2(Z_a + Z_0)$ has been factored out from numerator and denominator. It is observed that (10) is exactly the Z_{ANT} expressed

by (1) under the condition $Z_a = Z_b$. Therefore, there would be no difference for Z_{ANT} and Z_{dd11} when measuring a balanced antenna. From the above discussion, it is concluded that even with time consuming post-processing, Z_{ANT} gives accurate impedance for both balanced and unbalanced antennas. For a balanced antenna, Z_{dd11} is preferred since it can be directly obtained from the network analyzer equipped with mixed-mode parameter conversion.

4. MEASUREMENT RESULTS

In order to demonstrate the differential probe and the associated methods discussed in Section 3 is suitable for both balanced and unbalanced antennas, measurement results of two kinds of metal tags, namely loop antenna and patch antenna, are presented in this section. For the purpose of comparison, impedance measured by the single-ended probe shown in Fig. 2(a) and the balun connected probe shown in Fig. 2(b) are also presented.

4.1. Measurement of Loop Antenna

Metal tag made by a vertical small loop has miniature size and adequate read range for applications for metallic objects [9]. A slim shape RFID tag formed by a loop surrounding FR4 substrate can be attached to steel plate. Fig. 6(a) shows the tag has dimension $59 \times 4 \times 1.6 \text{ mm}^3$, which has 0.4m read range when place right on top of the metal surface. Fig. 6(b) shows the differential probe was

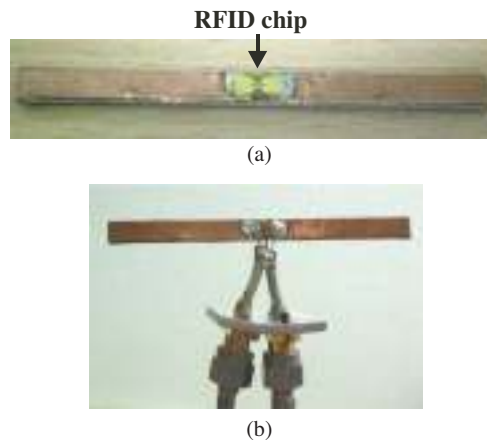


Figure 6. Measurement of a loop tag. (a) A loop antenna for metallic surface, (b) Probing the antenna with the differential probe.

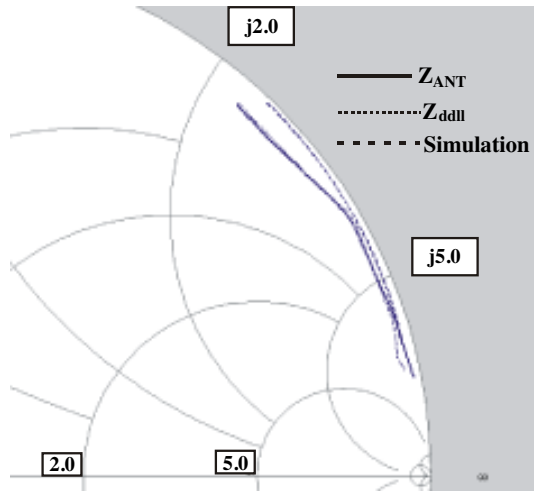


Figure 7. Measurement results of the loop antenna using the differential probe.

soldered to the loop during the measurement. The frequency sweep is set from 800 MHz to 1200 MHz during the measurement. It is seen that the measurement results as demonstrated in Fig. 7 agree with the simulation result. Because the loop antenna with symmetrical structure is considered as a balance load, the trace of both Z_{ANT} and Z_{dd11} are closely overlapped. Fig. 8 shows the measurement results using the two well-known probes presented in Section 2. It is observed that the balun probe provides better agreement than the single-ended probe. However, it also shows the balun probe has larger noise on the trace of the Smith Chart, which might be due to the surrounding noises pick up by the coil. The simulated and measured impedance values of specific frequency at 925 MHz are also listed in Table 1.

Table 1. Measurement and simulation results of the loop antenna at 925 MHz simulated impedance = $3.5 + j156.7 \Omega$.

	Measured Impedance	Deviation from simulation (%)
Z_{ANT}	$11.2 + j152.2 \Omega$	5.7%
Z_{dd11}	$11.1 + j151.6 \Omega$	5.8%
Balun	$15.6 + j159.8 \Omega$	8.0%

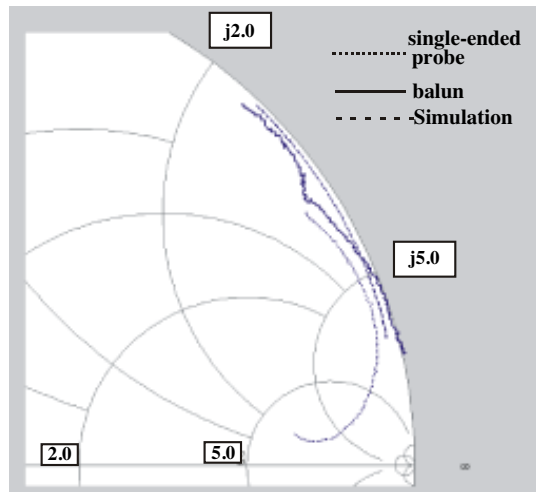


Figure 8. Measurement results of the loop antenna using conventional method.

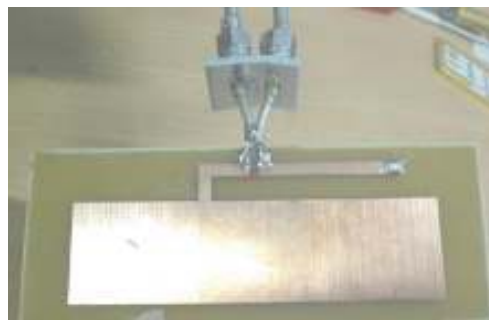


Figure 9. Measurement of a patch antenna.

4.2. Measurement of Patch Antenna

Patch antenna is employed for various applications because of its low profile [20, 21], miniature size and wide bandwidth features [22–25]. Most patch antennas are categorized as unbalanced antenna because of its unsymmetrical structure [26, 27]. A patch antenna for the purpose of RFID tag on metal application is designed. Fig. 9 shows the patch antenna probed by the differential probe. The developed patch antenna has a dimension $100 \times 40 \times 1.6 \text{ mm}^3$, with a rectangular patch and feed position on the front surface of the FR4 substrate. A calibration process based on fitting resonance frequency of a 50 Ohm patch antenna

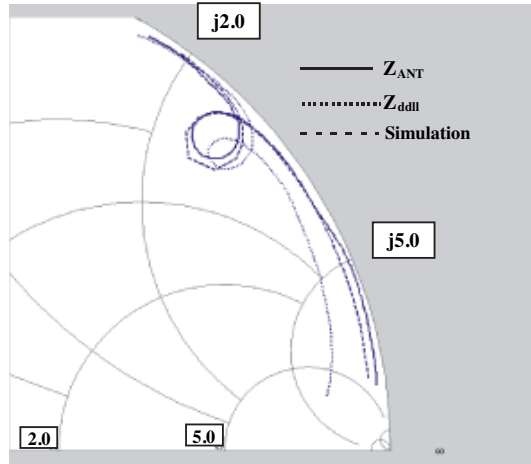


Figure 10. Measurement results of the patch antenna using the differential probe.

was employed to calibrate the dielectric constant and loss tangent [9], which are found to be 4.28 and 0.018, respectively. The patch metal tag has a read range around 1.4 m when placed on metal plate and 2.0 m in the air. The design and simulation was performed using Ansoft HFSS to achieve impedance $7.2 + j127.7$ at 925 MHz, close to the conjugate impedance value $11 - j131$ of Alien UHF chip. Measurement results of Z_{ANT} and Z_{dd11} , along with simulation result are demonstrated in Fig. 10. It is observed that Z_{ANT} is closer to the simulated impedance over the entire frequency sweeping range. The difference between Z_{ANT} and Z_{dd11} is mainly due the unbalanced nature of the patch antenna, which can be verified in Fig. 11 in which Z_a and Z_b are different from each other over the entire sweep frequencies.

Table 2. Measurement and simulation results of the patch antenna at 925 MHz simulated impedance = $7.2 + j127.7 \Omega$.

	Measured Impedance	Deviation from simulation (%)
Z_{ANT}	$8.9 + j118.6 \Omega$	7.2%
Z_{dd11}	$20.0 + j122.5 \Omega$	10.8%
Balun	$15.7 + j135.8 \Omega$	9.2%

For the single-ended probe, the measurement is setup in two ways so that the feed extended from the patch can be connected either to the

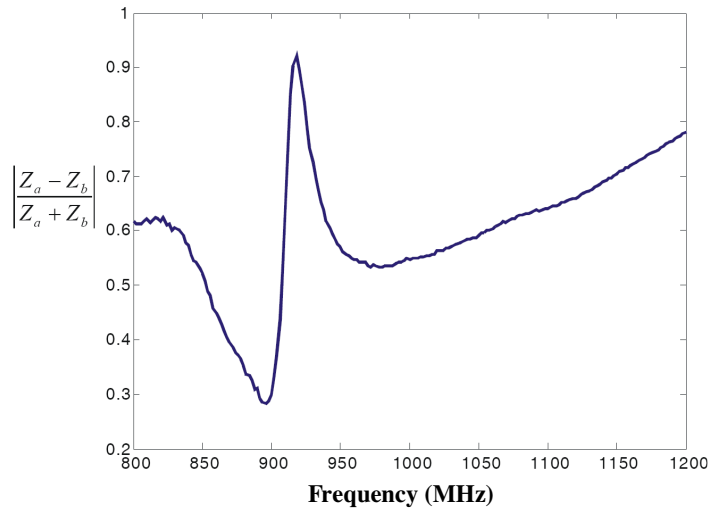


Figure 11. Evaluation of unbalance of the patch antenna.

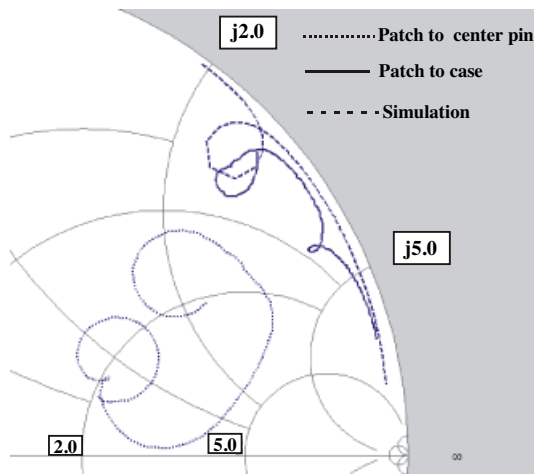


Figure 12. Measurement of the patch antenna using the single-ended probe.

center pin or to the case. The measured results illustrated in Fig. 12 showing unacceptable measurement errors. On the other hand, Fig. 13 shows the trace given by the balun probe has better agreement with simulation. However, the noise induced by the coil is clearly identified. Table 2 compares deviation of measurement results from simulation.

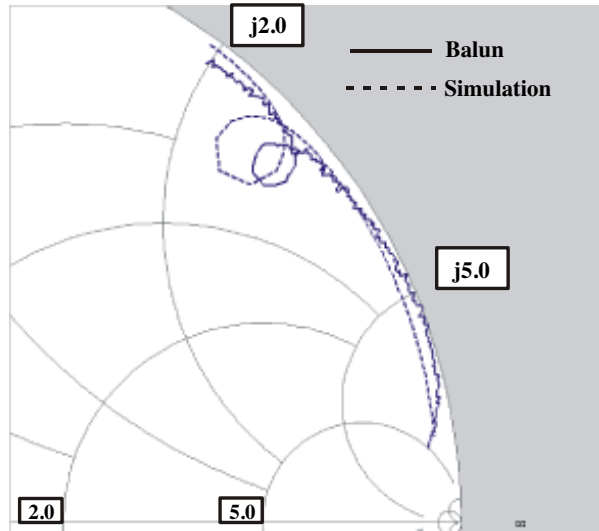


Figure 13. Measurement of the patch antenna using the balun probe.

5. CONCLUSIONS

An accurate and reliable impedance measurement result highly relies on the configuration of the probe. Since the differential probe has a balanced structure, the imposed measurement error would be minimized. Experiment results clearly prove that the performance of the impedance measurement method based on differential probe has better accuracy and noise immunity than the single ended probe and the balun probe.

REFERENCES

1. Fan, Z. G., S. Qiao, J. T. Huangfu, and L. X. Ran, "A miniaturized printed dipoles for 2.45 GHz RFID readers," *Progress In Electromagnetics Research*, PIER 71, 149–158, 2007.
2. Kim, D.-Y. and J.-G. Yook, "Interference analysis of UHF RFID systems," *Progress In Electromagnetics Research B*, Vol. 4, 115–126, 2008.
3. Shi, X.-L., X.-W. Shi, Q.-L. Huang, and F. Wei, "An enhanced binary anti-collision algorithm of backtracking in RFID system," *Progress In Electromagnetics Research B*, Vol. 4, 263–271, 2008.
4. Ng, M. L., K. S. Leong, and P. H. Cole, "Design and

- miniaturization of an RFID tag using a simple rectangular patch antenna for metallic object identification,” *IEEE Antennas and Propagation Society International Symposium*, 1741–1744, Hawaii, USA, 2007.
5. Park, Y., S. Lee, J. Kang, and Y. C. Chung, “Various UHF RFID tag for metallic object,” *IEEE Antennas and Propagation Society International Symposium*, 2285–2288, Hawaii, USA, 2007.
 6. Ukkonen, L., M. Schaffrath, D. W. Engels, L. Sydänheimo, and M. Kivikoski, “Operability of folded microstrip patch-type tag antenna in the UHF RFID bands within 865–928 MHz,” *IEEE Antennas and Wireless Propagation Letters*, Vol. 5, No. 1, 414–417, Dec. 2006.
 7. Choi, W., H. W. Son, J.-H. Bae, G. Y. Choi, C. S. Pyo, and J.-S. Chae, “An RFID tag using a planar inverted-F antenna capable of being stuck to metallic objects,” *ETRI Journal*, Vol. 28, No. 2, Apr. 2006.
 8. Hirvonen, M., P. Pursula, K. Jaakkola, and K. Laukkanen, “Planar inverted-F antenna for radio frequency identification,” *Electronic Letters*, Vol. 40, No. 14, Jul. 2004.
 9. Ng, M. L., K. S. Leong, and P. H. Cole, “A small passive UHF RFID tag for metallic item identification,” *International Technical Conference on Circuits/Systems, Computers and Communications*, 10–13, Chiang Mai, Thailand, Jul. 2006.
 10. Loo, C.-H., K. Elmahgoub, F. Yang, A. Elsherbeni, D. Kajfez, A. Kishk, T. Elsherbeni, L. Ukkonen, L. Sydänheimo, M. Kivikoski, S. Merilampi, and P. Ruuskanen, “Chip impedance matching for UHF RFID tag antenna design,” *Progress In Electromagnetics Research*, PIER 81, 359–370, 2008.
 11. Stutzman, W. L. and G. A. Thiele, *Antenna Theory and Design*, John Wiley & Sons, 1998.
 12. Leong, K. S., M. N. Mg, and P. H. Cole, “Investigation of RF cable effect on RFID tag antenna impedance measurement,” *IEEE Antennas and Propagation Society International Symposium*, 573–576, Hawaii, USA, 2007.
 13. Eunni, M. B., “A novel planar microstrip antenna design for UHF RFID,” M.S. Thesis, University of Kansas, Jul. 2006.
 14. Camp, M., R. Herschman, T. Zelder, and H. Eul, “Determination of the input impedance of RFID transponder antennas with novel measurement procedure using a modified on-wafer-prober,” *Advances in Radio Science*, Vol. 5, 115–118, 2007.
 15. Yang, Z. Q., T. Yang, and Y. Liu, “Analysis and design of a

- reduced-size marchand balun,” *Journal of Electromagnetic Waves and Applications*, Vol. 21, No. 9, 1169–1175, 2007.
16. Dobkin, D. M. and S. M. Weigand, “Environmental effects on RFID tag antennas,” *Microwave Symposium Digest, 2005 IEEE MTT-S International*, Jun. 12–17, 2005.
 17. Palmer, K. D. and M. W. Rooyen, “Simple broadband measurements of balanced loads using a network analyzer,” *IEEE Transactions on Instrumentation and Measurement*, Vol. 55, No. 1, 266–272, Feb. 2006.
 18. Fan, W., A. Lu, L. L. Wai, and B. K. Lok, “Mixed-mode S -parameter characterization of differential structures,” *Electronics Packaging Technology, 5th Conference*, 533–537, Dec. 10–12, 2003.
 19. “Single-ended and differential S -parameters,” MAXIM application note, hfan-5.1.0.
 20. Elsadek, H. and D. Nashaat, “Ultra mimiturized E-shaped dual band PIFA on cheap foam and FR4 substrate,” *Journal of Electromagnetic Waves and Applications*, Vol. 20, No. 3, 291–300, 2006.
 21. Zhang, M. T., Y. B. Chen, Y. C. Jiao, and F. S. Zhang, “Dual circularly polarized antenna of compact structure for RFID application,” *Journal of Electromagnetic Waves and Applications*, Vol. 20, No. 14, 1895–1902, 2006.
 22. Sim, C. Y. D., “A novel dual frequency PIFA design for ease of manufacturing,” *Journal of Electromagnetic Waves and Applications*, Vol. 21, No. 3, 409–419, 2007.
 23. Elsadek, H. and D. Nashaat, “Quad band compact size trapezoidal PIFA antenna,” *Journal of Electromagnetic Waves and Applications*, Vol. 21, No. 7, 865–876, 2007.
 24. Khodaei, G. F., J. Nourinia, and C. Ghobadi, “A practical miniaturized U-slot patch antenna with enhanced bandwidth,” *Progress In Electromagnetics Research B*, Vol. 3, 47–62, 2008.
 25. Abbaspour, M. and H. R. Hassani, “Wideband star-shaped microstrip patch antenna,” *Progress In Electromagnetics Research Letters*, Vol. 1, 61–68, 2008.
 26. Jolani, F. and A. M. Dadgarpour, “Compact M-slot folded patch antenna for WLAN,” *Progress In Electromagnetics Research Letters*, Vol. 3, 35–42, 2008.
 27. Mahmoud, S. F. and A. F. Sheta, “Cavity mode analysis for a rectangular patch with a shorting pin,” *Journal of Electromagnetic Waves and Applications*, Vol. 20, No. 14, 2013–2025, 2006.